Neutron star properties from modern meson-exchange potential models

G. Bao ^a, L. Engvik ^b, M. Hjorth-Jensen ^b, E. Osnes ^band E. Østgaard ^a

Abstract: In this work we calculate the total mass, radius, moment of inertia, and surface gravitational redshift for neutron stars using various equations of state (EOS). The latter are derived from the recent meson-exchange potential models of the Bonn group, and we derive both a non-relativistic and a relativistic EOS. Of importance here is the fact that relativistic Brueckner-Hartree-Fock calculations for symmetric nuclear matter meet the empirical data, which are not reproduced by non-relativistic calculations. Relativistic effects are known to be important at high densities, giving an increased repulsion. This leads to a stiffer EOS compared to the EOS derived with a non-relativistic approach. Both the non-relativistic and the relativistic EOS yield values for moment of inertia and redshifts in agreement with the accepted values. The relativistic EOS yields however too large mass and radius. The implications are discussed.

1 Introduction

The physics of compact objects like neutron stars offers an intriguing interplay between nuclear processes and astrophysical observables [1,2]. Neutron stars exhibit conditions far from those encountered on earth; typically, expected densities ρ of a neutron star interior are of the order of 10^3 or more times the density at neutron "drip" $\rho_d \approx 4 \cdot 10^{11} \text{ g/cm}^3$. Thus, the determination of an equation of state for dense matter is central to calculations of neutron star properties, and it determines the mass range as well as the mass-radius relationship for these stars. It is also an important ingredient in the determination of the composition of dense matter and the thickness of the crust in a neutron star. The latter influences neutrino generating processes and the cooling of neutron stars [3]. In addition, a theoretical result for the maximum mass

a Department of Physics, AVH, University of Trondheim, N-7055 Dragvoll, Norway

^b Department of Physics, University of Oslo, N-0316 Oslo, Norway

of neutron stars will have very important astrophysical implications for the existence and number of black holes in the universe, examples are the famous galactic black hole candidates Cyg X-1 and LMC X-3. If the maximum mass of a neutron star gets smaller, the probability for getting a black hole after a supernova should become larger.

Important in this study is the derivation of the equation of state (EOS), i.e. the functional dependence of the pressure P on density ρ , for dense neutron matter from the underlying many-body theory, derived from a realistic nucleonnucleon (NN) interaction. By realistic we shall mean a nucleon-nucleon interaction defined within the framework of meson-exchange theory, described conventionally in terms of one-boson-exchange (OBE) models [4,5]. Explicitly, we will here build on the Bonn meson-exchange potential models as they are defined in table A.2 of ref. [4]. Further, the physically motivated coupling constants and energy cut-offs which determine the OBE potentials are constrained through a fit to the available scattering data. The subsequent step is to obtain an effective NN interaction in the nuclear medium by solving the Bethe-Goldstone equation self-consistently. Thus, the only parameters which enter the theory are those which define the NN potential. Such an approach is commonly referred to as parameter-free in order to distinguish it from methods where the meson masses and coupling constants are adjusted to the bulk nuclear matter properties [2,6].

Until recently, most microscopic calculations of the EOS for nuclear or neutron matter have been carried out within a non-relativistic framework [7], where the non-relativistic Schrödinger equation is used to describe the singleparticle motion in the nuclear medium. Various degrees of sophistication are accounted for in the literature [1,4], ranging from first-order calculations in the reaction matrix G to the inclusion of two- and three-body higher-order effects [4,7–9]. A common problem to non-relativistic nuclear matter calculations is, however, the simultaneous reproduction of both the binding energy per nucleon $(BE/A = -16 \pm 1 \text{ MeV})$ and the saturation density with a Fermi momentum $k_F = 1.35 \pm 0.05 \text{ fm}^{-1}$. Results obtained with a variety of methods and nucleon-nucleon (NN) interactions are located along a band denoted the "Coester band", which does not satisfy the empirical data for nuclear matter. Albeit these deficiencies, much progress has been achieved recently in the description of the saturation properties of nuclear matter. Of special relevance is the replacement of the non-relativistic Schrödinger equation with the Dirac equation to describe the single-particle motion, referred to as the Dirac-Brueckner (DB) approach. This is motivated by the success of the phenomenological Dirac approach in nucleon-nucleus scattering [10] and in the description of properties of finite nuclei [11], such as the spin-orbit splitting in finite nuclei [12]. Moreover, rather promising results within the framework of the DB approach have been obtained by Machleidt, Brockmann and Müther [13–15], employing the OBE models of the Bonn group. Actually, the empirical properties of nuclear matter are quantitatively reproduced by Brockmann and Machleidt [13].

This work falls in four sections. After the introductory remarks, we briefly review the general picture in section 2. In this section we also recast some of the astrophysical equations, together with the equations of state derived within both the non-relativistic and the Dirac-Brueckner-Hartree-Fock approaches. The results are presented in section 3, while discussions and conclusions are given in section 4.

2 General Theory

In the interior of neutron stars, we find matter at densities above the neutron "drip" ρ_d , and the properties of cold dense matter and the associated equation of state are reasonably well understood at densities up to $\rho_n \approx 3 \cdot 10^{14} \text{g/cm}^3$, the density at which nuclei begin to dissolve and merge together. In the high-density range above ρ_n the physical properties of matter are still uncertain.

In the region between ρ_d and ρ_n matter is composed mainly of nuclei, electrons and free neutrons. The nuclei disappear at the upper end of this density range because their binding energy decreases with increasing density. The nuclei then become more neutron-rich and their stability decreases until a critical value of the neutron number is reached, at which point the nuclei dissolve, essentially by merging together. Since the nuclei present are very neutron-rich, the matter inside nuclei is very similar to the free neutron gas outside. However, the external neutron gas reduces the nuclear surface energy appreciably, and it must vanish when the matter inside nuclei becomes identical to that outside.

The free neutrons supply an increasingly larger fraction of the total pressure as the density increases, and at neutron drip the pressure is almost entirely due to neutrons. Slightly above neutron drip the adiabatic index drops sharply since the low-density neutron gas contributes appreciably to the density but not much to the pressure, and it does not rise again above 4/3 until $\rho > 7 \cdot 10^{12}$ g/cm³. This means that no stable stars can have central densities in this region.

Relatively "soft" equations of state have been proposed since the average system energy is attractive at nuclear densities. However, "stiff" equations of state may result from potentials for which the average system interaction energy is dominated by the attractive part of the potential at nuclear densities, but by the repulsive part at higher densities. The stiffer equations of state give rise to important changes in the structure and masses of heavy neutron stars. As the interaction energy becomes repulsive above nuclear densities, the corresponding pressure forces are better able to support stellar matter

against gravitational collapse. The result is that the maximum masses of stars based on stiff equations of state are greater than those based on soft equations of state. Also, stellar models based on stiffer equations have a lower central density, a larger radius and thicker crust. Such differences are important in determining mass limits for neutron stars, their surface properties, moment of inertia, etc.

For low densities $\rho < \rho_n$, where the nuclear force is expected to be attractive, the pressure is softened somewhat by the inclusion of interactions. For very high densities, however, the equation of state is hardened due to the dominance of the repulsive core in the nuclear potential.

At very high densities above 10^{15} g/cm³, the composition is expected to include an appreciable number of hyperons and the nucleon interactions must be treated relativistically. Relativistic many-body techniques for strongly interacting matter are, however, not fully developed. Presently developed nuclear equations of state are also subject to many uncertainties, such as the possibility of neutron and proton superfluidity, of pion or kaon condensation, of neutron solidification, of phase transitions to "quark matter", and the consequences of the \triangle nucleon resonance.

At densities significantly greater than ρ_n , it is no longer possible to describe nuclear matter in terms of a non-relativistic many-body Schrödinger equation. The "meson clouds" surrounding the nucleons begin to overlap and the picture of localized individual particles interacting via two-body forces becomes invalid. Even before this "break-down" different potentials which reproduce reliably low-energy phase shift data result in different equations of state, since the potentials are sensitive to the repulsive core region unaffected by the phase-shift data. If the fundamental building blocks of all strongly interacting particles are quarks, any description of nuclear matter at very high densities should involve quarks. When nuclei begin to "touch", matter just above this density should undergo a phase transition at which quarks would begin to "drip" out of the nucleons and the result would be quark matter, a degenerate Fermi liquid.

The main uncertainty in neutron star models is the equation of state of nuclear matter, particularly above typical nuclear densities of $\rho \sim 2.8 \cdot 10^{14} \text{ g/cm}^3$. But our present understanding of the condensed matter is already sufficient to place quite strict limits on masses and radii of stable neutron stars.

Neutron star models including realistic equations of state give the following general result: Stars calculated with a stiff equation of state have a lower central density, a larger radius, and a much thicker crust than stars of the same mass computed from a soft equation of state. Pion or kaon condensation and quark matter would tend to contract neutron stars of a given mass and

decrease the maximum mass.

Calculations give the following configurations in the interior: The surface for $\rho < 10^6 \,\mathrm{g/cm^3}$ is a region in which temperatures and magnetic fields may affect the equation of state. The outer crust for $10^6 \,\mathrm{g/cm^3} < \rho < 4 \cdot 10^{11} \,\mathrm{g/cm^3}$ is a solid region where a Coulomb lattice of heavy nuclei coexist in β -equilibrium with a relativistic degenerate electron gas. The inner crust for $4 \cdot 10^{11} \,\mathrm{g/cm^3} < \rho < 2 \cdot 10^{14} \,\mathrm{g/cm^3}$ consists of a lattice of neutron-rich nuclei together with a superfluid neutron gas and an electron gas. The neutron liquid for $2 \cdot 10^{14} \,\mathrm{g/cm^3} < \rho < 8 \cdot 10^{14} \,\mathrm{g/cm^3}$ contains mainly superfluid neutrons with a smaller concentration of superfluid protons and normal electrons. The core region for $\rho > 8 \cdot 10^{14} \,\mathrm{g/cm^3}$ may not exist in some stars and will depend on the existence of pion or kaon condensation, neutron solid, quark matter, etc. The existence of "quark stars" also remains a possibility.

The minimum mass of a stable neutron star is determined by setting the mean value of the adiabatic index Γ equal to the critical value for radial stability against collapse. The resulting minimum mass is $M \sim 0.1 M_{\odot}$, where M_{\odot} is the solar mass, with a corresponding central density of $\rho \sim 10^{14} \text{ g/cm}^3$ and radius $R \sim 200 \text{ km}$. The maximum mass equilibrium configuration is somewhat uncertain, but all microscopic calculations give $M < 2.7 M_{\odot}$.

Astronomical observations leading to global neutron star parameters such as total mass, radius, or moment of inertia, are important since they are sensitive to microscopic model calculations. The most reliable way of determining masses is via Kepler's third law in binary pulsars. Observations of such pulsars give approximately a common mass region consistent with all data of $1.2M_{\odot} < M < 1.8M_{\odot}$. Present mass determinations for neutron stars are all consistent with present stellar evolution theories.

A general limit for the maximum mass can be estimated by assuming the following: General relativity is the correct theory of gravitation. The equation of state must satisfy the "microscopic stability" condition $dP/d\rho \geq 0$ and the causality condition $dP/d\rho < c^2$, and should match some known low-density equation of state. This gives an upper limit of $M \sim 3-5M_{\odot}$. Stiff equations of state in calculations predict a maximum mass in the range $M \sim 1.5-2.7M_{\odot}$. Rotation may increase the maximum neutron star mass, but not appreciably, i.e., < 20%.

We aim here at discriminating between equations of state for pure neutron matter derived from non-relativistic and relativistic approaches (to be discussed below). As discussed above, relativistic effects become important at densities higher than ρ_n , and it is therefore of interest to understand whether the two approaches yield significantly different neutron star properties. The derivation of the equations of state is discussed in the first subsection, whereas

the equations which define the calculations of mass, radius, moment of inertia and gravitational redshifts are discussed in the subsequent subsection.

2.1 Derivation of the equation of state for neutron matter

A determination of the equation of state for neutron matter from the underlying many-body theory has been the subject of much effort for many years without a general consensus [16,17] on its behaviour at densities higher than the density of normal nuclear matter. It is, however, hoped that bulk properties of neutron stars as those discussed in the previous section, can shed some light on the functional dependence of the energy per particle \mathcal{E}/A .

In this subsection we discuss both a non-relativistic and a relativistic equation of state for neutron matter within the framework of the Brueckner-Hartree-Fock (BHF) approach. Especially, in this work we study the BHF approach as it is approximated by the model-space BHF method of Kuo and Ma [9].

2.1.1 The model-space Brueckner-Hartree-Fock approach

The basic formalism behind the model-space BHF approach has been exposed elsewhere, see e.g., refs. [9,19,20], thus we will here only briefly sketch the essential ingredients which enter our calculations.

Following the conventional many-body approach, we divide the full hamiltonian H = T + V, with T being the kinetic energy and V the bare NN potential, into an unperturbed part $H_0 = T + U$ and an interacting part $H_I = V - U$, such that

$$H = T + V = H_0 + H_I,$$

where we have introduced an auxiliary single-particle (sp) potential U. If U is chosen such that H_I becomes small, then perturbative many-body techniques can presumably be applied. A serious obstacle to any perturbative treatment is the fact that the bare NN potential V is very large at short inter-nucleonic distances, which renders a perturbative approach highly prohibitive. To overcome this problem, we introduce the reaction matrix G given by the solution of the Bethe-Goldstone equation (in operator form)

$$G(E) = V + VQ \frac{1}{E - QH_0Q} QG, \tag{1}$$

where E is the energy of the interacting nucleons and Q is the Pauli operator which prevents scattering into occupied states. More explicitly, the above

equation reads (in a partial wave representation)

$$G_{ll'}^{\alpha}(kk'KE) = V_{ll'}^{\alpha}(kk') + \sum_{l''} \int \frac{d^3q}{(2\pi)^3} V_{ll''}^{\alpha}(kq) \frac{Q(q,K)}{E - H_0} G_{l''l'}^{\alpha}(qk'KE), \qquad (2)$$

with ll' and kk' the orbital angular momentum and the linear momentum of the relative motion, respectively. K is the momentum of the center-of-mass motion. Since we are going to use an angular average for the Pauli operator, the G-matrix is diagonal in total angular momentum I and orbital angular momentum I for the center-of-mass motion. Further, the I-matrix is diagonal in isospin I and spin I. These quantities, i.e. I, I, I, I and I, are all represented by the variable I. The term I-I0 in the denominator of eq. (2) is the unperturbed energy of the intermediate states, and I1 is the corresponding momentum of the center-of-mass motion. I1 depends on both I2 and I3, see discussion below. The I3-matrix elements are anti-symmetrized.

The choice of the Pauli operator is decisive to the determination of the sp spectrum. Basically, to first order in the reaction matrix G there are three commonly used sp spectra, all defined by the self-consistent solution of the following equations

$$\varepsilon_{\alpha} = \varepsilon(k_{\alpha}) = t_{\alpha} + u_{\alpha} = \frac{k_{\alpha}^2}{2m} + u_{\alpha},$$
 (3)

where m is the bare nucleon mass, and

$$u_{\alpha} = \sum_{h \le k_F} \langle \alpha h | G(\omega = \varepsilon_{\alpha} + \varepsilon_h) | \alpha h \rangle_{AS}, \ k \le k_M,$$
(4)

$$u_k = 0, k > k_M.$$

For notational economy, we set $|\mathbf{k}_{\alpha}| = k_{\alpha}$. Here we use anti-symmetrized matrix elements (AS), and k_M is a cut-off on the momentum. t_{α} is the sp kinetic energy and similarly u_{α} is the sp potential. The choice of cut-off k_M is actually what determines the three commonly used sp spectra. In the conventional BHF approach one takes $k_M = k_F$, which leads to a Pauli operator $Q_{\rm BHF}$ (in the laboratory system) given by

$$Q_{\text{BHF}}(k_m, k_n) = \begin{cases} 1, & \min(k_m, k_n) > k_F, \\ 0, & otherwise. \end{cases}$$
 (5)

The BHF choice sets $u_k = 0$ for $k > k_F$, which leads to an unphysically large gap at the Fermi surface. To overcome this problem, Mahaux and collaborators

[18] introduced a continuous sp spectrum for all values of k, i.e. they set $k_M = \infty$. The divergencies which then may occur in eq. (1) are taken care of by introducing a principal value integration in eq. (1), to retain only the real part contribution to the G-matrix.

Finally, the model-space BHF approach which we shall employ, adopts a cutoff $k_M = ak_F$, where a is a constant. Thus, the cut-off k_M is given as a multiple of the Fermi momentum. A frequently used value [9] is a = 2, a choice also used here. This means that we extend the BHF spectrum to go beyond k_F . The resulting Pauli operator $Q_{\rm MBHF}$ (in the laboratory system) for the modelspace BHF method is

$$Q_{\text{MBHF}}(k_m, k_n) = \begin{cases} 1, & \min(k_m, k_n) > k_F \quad and \quad \max(k_m, k_n) > k_M, \\ 0, & otherwise. \end{cases}$$
(6)

If we set $k_M = k_F$, we obtain the traditional BHF choice. Since we use an angle-average approximation to the Pauli operator, it is convenient to transform the Pauli operator from the laboratory frame of reference to that of the center-of-mass and relative motion. For these details, we refer the reader to refs. [9,19].

In connection with the model-space BHF method, it is worth noting the following: Relating the model-space BHF approach to the conventional BHF sp spectrum and the continuous sp spectrum, we may say that the model-space BHF is an intermediate scheme in the sense that we introduce an extended Pauli operator in eq. (6) such that we have a continuous sp spectrum for $k < k_M$, while for $k > k_M$ the spectrum is that of a free particle. Moreover, the model-space BHF definition of the Pauli operator gives a G-matrix which does not account for scattering into intermediate states if both particles have momenta between k_F and k_M . This is, however, a welcome feature of the model-space BHF method as it allows one to consider collective excitations like the summation of particle-particle hole-hole (pp-hh) terms without double-counting problems [19]. Finally, a more general approach to eq. (4) would be to replace the G-matrix with the self-energy vertex function, which includes higher-order effects in G as well. However, as already pointed out above, we will limit our attention to G only.

It should be remarked that although we have removed the angle dependence of the Pauli operator, the energy denominator in eq. (2) still depends on the angle between the relative and center-of-mass momenta. This angle dependence is handled by the so-called effective mass approximation. The single-particle energies in nuclear matter are assumed to have the simple quadratic form

$$\varepsilon_{\alpha} = \frac{k_{\alpha}^{2}}{2m^{*}} + \Delta, \ k_{\alpha} \leq k_{M},$$

$$= \frac{k_{\alpha}^{2}}{2m}, \quad k_{\alpha} > k_{M},$$

$$(7)$$

where m^* is the non-relativistic effective mass of the nucleon and m is the bare nucleon mass. For particle states above k_M we choose a pure kinetic energy term, whereas for hole states the terms m^* and Δ (Δ is an effective single-particle potential related to the G-matrix) are obtained through the self-consistent Brueckner-Hartree-Fock (BHF) procedure. This self-consistency scheme consists in choosing adequate initial values of the effective mass and Δ . The obtained G-matrix is then used to obtain new values for m^* and Δ , and this procedure continues until these parameters show little variation. The starting energy E is then determined by the energy of the interacting nucleons, i.e.,

$$E = \frac{k^2}{m^*} + \frac{K^2}{4m^*} + 2\Delta.$$

Finally, the non-relativistic energy per particle \mathcal{E}/A is formally given as

$$\mathcal{E}/A = \frac{1}{A} \left\{ \sum_{h \le k_F} \frac{k_h^2}{2m} + \frac{1}{2} \sum_{hh' \le k_F} \langle hh' | G(E = \varepsilon_h + \varepsilon_{h'}) | hh' \rangle_{AS} \right\}.$$
 (8)

2.1.2 Relativistic effects

The properties of neutron stars depend on the equation of state at densities up to an order of magnitude higher than those observed in ordinary nuclei. At such densities, relativistic effects certainly prevail. Among relativistic approaches to the nuclear many-body problem, the so-called Dirac-Hartree and Dirac-Hartree-Fock approaches have received much interest. One of the early successes of these approaches was the quantitative reproduction of spin observables, which are only poorly described by the non-relativistic theory. Important to these methods was the introduction of a strongly attractive scalar component and a repulsive vector component [6,12] in the nucleon selfenergy. Inspired by the successes of the Dirac-Hartree-Fock method, a relativistic extension of Brueckner theory was proposed by the Brooklyn group [21], known as the Dirac-Brueckner theory. One of the appealing features of the Dirac-Brueckner approach is the self-consistent determination of the relativistic sp energies and wave functions. The Dirac-Brueckner approach differs from the Dirac-Hartree-Fock one in the sense that in the former one departs from the free NN potential which is only constrained by a fit to the NN data,

whereas the Dirac-Hartree-Fock method pursues a line where the parameters of the theory are determined so as to reproduce the bulk properties of nuclear matter. It ought, however, to be stressed that the Dirac-Brueckner approach [13,21,22], which starts from NN potentials based on meson exchange, is a non-renormalizable theory, where the short-range part of the potential depends on additional parameters like vertex cut-offs, clearly minimizing the sensitivity of calculated results to short-distance inputs. This should be contrasted to the Dirac-Hartree-Fock method pioneered by Walecka and Serot [6,23,24].

The description presented here for the Dirac-Brueckner approach follows closely that of Brockmann and Machleidt [13]. We will thus use the meson-exchange models of the Bonn group, defined in table A.2 of ref. [4]. There the three-dimensional reduction of the Bethe-Salpeter equation as given by the Thompson equation [25] is used to solve the equation for the scattering matrix. Hence, including the necessary medium effects like the Pauli operators discussed in the previous subsection and the starting energy, we will rewrite eq. (2) departing from the Thompson equation. Then, in a self-consistent way, we determine the above-mentioned scalar and vector components which define the nucleon self-energy. In this sense we also differ from the non-relativistic approach discussed above, where the parameters which are varied at each iterative step are the non-relativistic effective mass and the effective sp potential Δ .

In order to introduce the relativistic nomenclature, we consider first the Dirac equation for a free nucleon, i.e.,

$$(i \not \partial - m)\psi(x) = 0,$$

where m is the free nucleon mass and $\psi(x)$ is the nucleon field operator (x is a four-point) which is conventionally expanded in terms of plane wave states and the Dirac spinors u(p,s), and v(p,s), where $p=(p^0,\mathbf{p})$ is a four momentum ¹ and s is the spin projection.

The positive energy Dirac spinors are (with $\overline{u}u = 1$)

$$u(p,s) = \sqrt{\frac{E(p) + m}{2m}} \begin{pmatrix} \chi_s \\ \frac{\boldsymbol{\sigma} \cdot \mathbf{p}}{E(p) + m} \chi_s \end{pmatrix}, \tag{9}$$

where χ_s is the Pauli spinor and $E(p) = \sqrt{m^2 + |\mathbf{p}|^2}$. To account for medium modifications to the free Dirac equation, we introduce the notion of the self-energy $\Sigma(p)$. As we assume parity to be a good quantum number, the self-

¹ Further notation is as given in Itzykson and Zuber [26]. Moreover, hereafter we set $G = c = \hbar = 1$, where G is the gravitational constant.

energy of a nucleon can be formally written as

$$\Sigma(p) = \Sigma_S(p) - \gamma_0 \Sigma^0(p) + \gamma \mathbf{p} \Sigma^V(p).$$

The momentum dependence of Σ^0 and Σ_S is rather weak [6]. Moreover, $\Sigma^V << 1$, such that the features of the Dirac-Brueckner-Hartree-Fock procedure can be discussed within the framework of the phenomenological Dirac-Hartree ansatz, i.e. we approximate

$$\Sigma \approx \Sigma_S - \gamma_0 \Sigma^0 = U_S + U_V,$$

where U_S is an attractive scalar field and U_V is the time-like component of a repulsive vector field. The finite self-energy modifies the free Dirac spinors of eq. (9) as

$$\tilde{u}(p,s) = \sqrt{\frac{\tilde{E}(p) + \tilde{m}}{2\tilde{m}}} \begin{pmatrix} \chi_s \\ \frac{\boldsymbol{\sigma} \cdot \mathbf{p}}{\tilde{E}(p) + \tilde{m}} \chi_s \end{pmatrix},$$

where we let the terms with tilde represent the medium modified quantities. Here we have defined [6,13]

$$\tilde{m} = m + U_S$$

and

$$\tilde{E}_{\alpha} = \tilde{E}(p_{\alpha}) = \sqrt{\tilde{m}^2 + \mathbf{p}_{\alpha}^2}.$$

The relativistic analog of eq. (3) is [13]

$$\tilde{\varepsilon}_{\alpha} = \tilde{E}_{\alpha} + U_{V},\tag{10}$$

and the sp potential is given as

$$u_{\alpha} = \sum_{h \leq k_{\rm F}} \frac{\tilde{m}^2}{\tilde{E}_h \tilde{E}_{\alpha}} \langle \alpha h | \tilde{G}(\tilde{E} = \tilde{\varepsilon}_{\alpha} + \tilde{\varepsilon}_h) | \alpha h \rangle_{\rm AS}, \qquad (11)$$

or, if we wish to express it in terms of the constants U_S and U_V , we have

$$u_{\alpha} = \frac{\tilde{m}}{\tilde{E}_{\alpha}} U_S + U_V. \tag{12}$$

Eq. (7) becomes

$$\tilde{\varepsilon}_{\alpha} = \tilde{E}_{\alpha} + U_{V}, |\mathbf{p}_{\alpha}| \le k_{M},$$

$$= \tilde{E}_{\alpha}, |\mathbf{p}_{\alpha}| > k_{M},$$
(13)

where $k_M = k_F$ gives the traditional BHF sp spectrum while $k_M = ak_F$ with a > 1 results in the MBHF approach. In eq. (11), we have introduced the

relativistic \tilde{G} -matrix, which in a partial wave representation is given by

$$\tilde{G}_{ll'}^{\alpha}(kk'K\tilde{E}) = \tilde{V}_{ll'}^{\alpha}(kk') + \sum_{l''} \int \frac{d^3q}{(2\pi)^3} \tilde{V}_{ll''}^{\alpha}(kq) \frac{\tilde{m}^2}{\tilde{E}_{\frac{1}{2}K+q}^2} \frac{Q(q,K)}{\tilde{E} - 2\tilde{E}_{\frac{1}{2}K+q}} \tilde{G}_{l''l'}^{\alpha}(qk'K\tilde{E}),$$
(14)

where the relativistic starting energy is $\tilde{E} = 2\tilde{E}_{\frac{1}{2}K+k}$

Equations (10)-(14) are solved self-consistently in the same fashion as in the non-relativistic case, starting with adequate values for the scalar and vector components U_S and U_V . This iterative scheme is continued until these parameters show little variation. The calculations are carried out in the neutron matter rest frame, avoiding thereby a cumbersome transformation between the two-nucleon center-of-mass system and the neutron matter rest frame. The additional factors \tilde{m}/\tilde{E} in the above equations arise due to the normalization of the neutron matter spinors \tilde{w} , i.e. $\tilde{w}^{\dagger}\tilde{w}=1$ [13].

Finally, the relativistic version of eq. (8) reads

$$\mathcal{E}/A = \frac{1}{A} \left\{ \sum_{h \le k_F} \frac{\tilde{m}m + \mathbf{p}^2}{\tilde{E}_h} + \frac{1}{2} \sum_{hh' \le k_F} \frac{\tilde{m}^2}{\tilde{E}_h \tilde{E}_{h'}} \left\langle hh' \middle| \tilde{G}(\tilde{E} = \tilde{\varepsilon}_h + \tilde{\varepsilon}_{h'}) \middle| hh' \right\rangle_{AS} \right\} - m. \tag{15}$$

2.2 Neutron star equations

We end this section by presenting the formalism needed in order to calculate the mass, radius, moment of inertia and gravitational redshift. We will assume that the neutron stars we study exhibit an isotropic mass distribution. Hence, from the general theory of relativity, the structure of a neutron star is determined through the Tolman-Oppenheimer-Volkov eqs., i.e.,

$$\frac{dP}{dr} = -\frac{\{\rho(r) + P(r)\}\{M(r) + 4\pi r^3 P(r)\}}{r^2 - 2rM(r)},$$
(16)

and

$$\frac{dM}{dr} = 4\pi r^2 \rho(r),\tag{17}$$

where P(r) is the pressure, M(r) is the gravitional mass inside a radius r, and $\rho(r)$ is the mass energy density. The latter equation is conventionally written as an integral equation

$$M(r) = 4\pi \int_{0}^{r} \rho(r')r'^{2}dr'.$$
 (18)

In addition, the main ingredient in a calculation of astrophysical observables is the equation of state (EOS)

$$P(n) = n^2 \left(\frac{\partial \epsilon}{\partial n}\right),\tag{19}$$

where $\epsilon = \mathcal{E}/A$ is the energy per particle and n is the particle density. Eqs. (16), (18) and (19) are the basic ingredients in our calculations of neutron star properties.

The moment of inertia I for a slowly rotating symmetric neutron star is related to the angular momentum J and the angular velocity Ω in an inertial system at infinity through

$$I = \left(\frac{\partial J}{\partial \Omega}\right)_{\Omega = 0} = \frac{J}{\Omega}.\tag{20}$$

The metric outside a slowly rotating star is taken to be the Schwarzschild metric with an additional cross term

$$-2\omega r^2 \sin^2\theta d\phi dt$$
,

where $\omega(r)$ is the angular velocity of the local non-rotating system as measured by an observer in a far-away inertial system. In order to obtain the moment of inertia I, we need to calculate J and Ω in eq. (20). To obtain these quantities, we introduce the quantity

$$f(r) = 1 - \frac{\omega(r)}{\Omega},$$

we obtain

$$\frac{d}{dr}\left(r^4j(r)\frac{df}{dr}\right) + 4r^3\frac{dj}{dr}f(r) = 0,$$
(21)

where we have defined

$$j(r) = \sqrt{1 - 2M/r} \exp(-\nu(r)/2),$$

and the metric coefficient $\exp(-\nu(r)) = g_{00}$.

Integrating eq. (21) from r = 0 to r = R, assuming a spherical field in the vacuum outside the star and constraining the system to the boundary conditions $(\tilde{\omega} = \Omega - \omega)$, i.e.,

$$\tilde{\omega}(0) = const, \qquad \left(\frac{d\tilde{\omega}}{dr}\right)_{r=0} = 0,$$

we get

$$\tilde{\omega}(r) = \Omega - \frac{2J}{r^3}, \qquad r > R,$$
(22)

and

$$f(r) = 1 - \frac{2J}{r^3 \Omega}, \qquad r > R,$$
 (23)

leading to

$$\tilde{\omega}(\infty) = \Omega, \qquad f(\infty) = 1,$$
 (24)

and

$$J = \frac{1}{6}R^4 \left(\frac{d\tilde{\omega}}{dr}\right)_{r=R},\tag{25}$$

where $\tilde{\omega}$ is the angular velocity relative to particles with zero angular momentum.

The moment of inertia I follows from eq. (20). To get the angular momentum Ω , we define the quantity

$$u = r^4 \frac{d\tilde{\omega}}{dr},\tag{26}$$

and obtain

$$\frac{du}{dr} + \frac{d(\ln j)}{dr} \left(u + 4r^3 \tilde{\omega} \right) = 0, \tag{27}$$

and

$$\frac{d\tilde{\omega}}{dr} = \frac{u}{r^4}. (28)$$

For a given equation of state, we get

$$\frac{d\nu}{dr} = -2\left(\rho + P\right)^{-1} \frac{dP}{dr},\tag{29}$$

and Ω is calculated from u and $\tilde{\omega}$ with the result

$$\Omega = \tilde{\omega}(R) + \frac{u(R)}{3R^3}.$$
(30)

Finally, the gravitational redshift Z_s is given by

$$Z_s = \left(1 - \frac{2M(R)}{R}\right)^{-1/2} - 1. \tag{31}$$

To calculate the total mass, radius, moment of inertia and gravitational redshift, we employ the EOS defined in eq. (19) with the boundary conditions

$$P_c = P(n_c), \qquad M(0) = 0,$$

where we let the subscript c refer to the center of the star, and n_c is the central density which is our input parameter in the calculations of neutron star properties.

3 Results

3.1 The equation of state

As mentioned in the introduction, the replacement of the non-relativistic Schrödinger equation by the Dirac equation offers a quantitative reproduction of the saturation properties of nuclear matter [13]. Central to these results is the use of modern meson-exchange potentials with a weak tensor force, where the strength of the tensor force is reflected in the D-state probability of the deuteron. The main differences in the strength of the tensor force in nuclear matter arises in the T=0 ${}^3S_{1}$ ${}^3D_{1}$ channel, though other partial waves also give rise to tensor force contributions. To derive the equation of state, we start from the Bonn NN potential models as they are defined by the parameters of table A.2 in ref. [4]. These potentials are recognized by the labels A, B and C, with the former carrying the weakest tensor force. In neutron matter (T=1), however, the important ${}^{3}S_{1}$ - ${}^{3}D_{1}$ channel does not contribute to the energy per particle, and the difference between the various potentials is expected to be small. This is indeed the case, as reported by Li et al. [15] in a recent neutron matter calculation. We show the same result in the upper part of fig. 1. There we plot the BHF results using the non-relativistic Schrödinger equation to describe the sp motion, see the discussion in subsec. 2.1. On the scale of fig. 1, there is hardly any difference. Further, with the existing uncertainty of neutron star properties, the rather small differences between the energies derived from the Bonn A, B and C potentials are not expected to be significant, see also the discussion below. A similar conclusion is reached when we perform the relativistic model-space BHF calculations. Thus, in our presentation of neutron star properties, we will use the EOS derived from the Bonn A potential, mainly because this is the potential which gives the best reproduction of the saturation properties of nuclear matter. In the lower part of fig. 1 we compare first the non-relativistic BHF and MBHF results. As can be seen from the corresponding curves which are a solid line and a dashed line for the non-relativistic MBHF and BHF results, respectively, there is hardly any difference. This is again primarily due to the fact that we have no contributions from the ${}^{3}S_{1}$ - ${}^{3}D_{1}$ channel in neutron matter. Actually, nuclear matter calculations with the MBHF method [9,27] show that the most significant difference between the MBHF and BHF approaches arises in the ${}^{3}S_{1}$ - ${}^{3}D_{1}$ channel, with differences of the order of 2 MeV. This can be understood from the fact that the MBHF approach with $k_M > k_F$ introduces intermediate state contributions of shorter range, contributions which are predominantly accounted for by the 3S_1 - 3D_1 channel. The fact that the MBHF and the BHF approaches give similar results for neutron matter is a gratifying property, though the

Fig. 1. Energy per neutron E/A as function of density n for various many-body approaches. The upper part of the figure shows results obtained with the non-relativistic BHF approach for the Bonn A (solid line), B (dashed line) and C (dotted line) potentials. In the lower part non-relativistic MBHF (solid line), non-relativistic BHF (dashed line) and relativistic MBHF (dotted line) results are shown. All the last results have been obtained with the Bonn A potential.

MBHF method ² is to be preferred since it allows for a consistent treatment of higher-order contributions in the perturbative expansion, such as the summation of the particle-particle-hole-hole ring diagrams without double-counting problems. The investigations of such effects are the scope of a future work. Here we limit our attention to first order in the interaction G. However, the most important contribution from ring diagrams stems from the ${}^{3}S_{1}$ - ${}^{3}D_{1}$ channel, which is absent in our neutron matter model. Thus, the most significant

² The equations of state we will employ in the derivation of neutron star properties have all been obtained with the MBHF approach, both the non-relativistic and the relativistic EOS.

differences between various equations of state, are due to relativistic effects. This is clearly seen from the lower part of fig. 1. The relativistic MBHF calculation gives an increased repulsion at higher densities and correspondingly stiffer EOS than the non-relativistic approaches. In this figure we plot only the relativistic MBHF results, since they are similar to the relativistic BHF results³, in analogy to the non-relativistic results discussed above. Using the non-relativistic and the relativistic equations of state, we wish to study how these two extremes reproduce various neutron star properties. Note also that within the Dirac-Brueckner approach, the Bonn A potential reproduces the empirical nuclear matter binding energy and saturation density [13]. This gives a more consistent approach to pure neutron matter. The reader should however keep in mind that there are several mechanisms (to be discussed in section 4) which may reduce the stiffness of the above equations of state.

The equation of state can then easily be obtained through the use of eq. (19). The pressure can also be fitted numerically by the following polynomials;

$$P(n) = 0.048376 \times n^{4/3} - 0.036764 \times n^{5/3} + 4.959151 \times n^{2}$$
$$-21.095163 \times n^{7/3} + 32.922084 \times n^{8/3} - 14.213806 \times n^{3}, \tag{32}$$

for the non-relativistic EOS with the Bonn A potential obtained with the MBHF approach, and

$$P(n) = -1271.125 \times n^{4/3} + 2010.914 \times n^{5/3} + 29279.687 \times n^{2}$$

$$-59189.0540 \times n^{7/3} - 403313.402 \times n^{8/3} + 2067381.296 \times n^{3}$$

$$-4162678.316 \times n^{10/3} + 4400107.684 \times n^{11/3}$$

$$-2422293.924 \times n^{4} + 550123.976 \times n^{13/3},$$
(33)

for the relativistic EOS obtained with the MBHF approach. The pressure is given in units of $[10^{34} \text{ N/m}^2]$. The range of validity for these two equations of state is $0.1 \text{ fm}^{-3} \leq n \leq 0.8 \text{fm}^{-3}$.

3.2 Mass, radius, moment of inertia and surface gravitational redshift

To calculate mass, radius, moment of inertia and surface gravitational redshift we need the EOS for all relevant densities. The equations of state derived in the previous subsection have a limited range, $0.1~{\rm fm^{-3}} \le n \le 0.8 {\rm fm^{-3}}$. We must therefore include equations of state for other densities as well. These equations of state are discussed below.

For the lowest densities, we use the Haensel-Zdunik-Dobaczewski (HZD) [28] equation of state. This equation of state is obtained in the following way: The

³ Our relativistic results are also similar to those reported by Li *et al.* [15].

pressure is fitted by a polynomial consisting of 9 terms, i.e.,

$$P(X) = \sum_{i=1}^{9} C_i X^{l_i}, \tag{34}$$

where

$$X = 1.6749 \times 10^5 n, (35)$$

n is given in [fm⁻³], and the values

$$n = 0.077, 0.154, 0.395, 0.762, 1.575, 3.147, 6.443, 12.240, 26.551,$$

in $[10^{-5}/\text{fm}^3]$, are chosen to give the coefficients C_i . The corresponding equations are solved by matrix inversion, and we obtain

$$P(X) = 8.471521942X^{1/3} - 40.437728191X^{2/3} + 74.927783479X$$
$$-67.102601796X^{4/3} + 30.011422630X^{5/3} - 4.207322319X^{2}$$
$$-1.419954871X^{7/3} + 0.589441363X^{8/3} - 0.060468689X^{3},$$
(36)

where P(X) is given in units of $[10^{27} \text{ N/m}^2]$ and in the density range of $2 \times 10^{-6} \text{ fm}^{-3} < n < 2.84 \times 10^{-4} \text{ fm}^{-3}$. We need all the decimals in the different terms to get an accuracy of at least two decimals in the net equation.

The Baym-Bethe-Pethick (BBP) [29] equations of state are taken from Øvergård and Østgaard [30]. The given data are fitted by two five-term polynomials to give (BBP-1)

$$P(n) = 4.3591n^{4/3} - 122.4841n^{5/3} + 1315.2746n^2 - 6180.0702n^{7/3} + 10659.0049n^{8/3},$$
(37)

where P(n) is given in units of $[10^{34} \text{ N/m}^2]$ for n in the density range of $0.00027 \text{ fm}^{-3} < n < 0.0089 \text{ fm}^{-3}$, and (BBP-2)

$$P(n) = 0.092718n^{4/3} - 0.035382n^{5/3} + 1.193525n^2 - 2.424555n^{7/3} + 2.472867n^{8/3},$$
(38)

where P(n) is given in units of $[10^{34} \text{ N/m}^2]$ for n in the density range of 0.0089 fm⁻³ < $n < 0.3 \text{ fm}^{-3}$.

The Arntsen- Øvergård (AØ-5) [30] equation of state is given by a five-term polynomial, i.e.,

$$P(n) = 9.4433n^{5/3} - 34.6909n^2 + 102.6575n^{8/3}$$
$$-87.6158n^3 + 14.3549n^{11/3},$$
 (39)

where P(n) is given in units of $[10^{34} \text{ N/m}^2]$ for n in the density range of 0.4 fm⁻³ < n < 3.6 fm⁻³.

The Pandharipande - Smith (PS) [31] equation of state is taken from Øvergård and Østgaard [30]. The given data are fitted by a five-term polynomial to give

$$P(n) = 4.0378n^{4/3} - 27.853n^{5/3} + 52.0859n^2$$
$$-20.7073n^{7/3} + 5.5808n^{8/3}.$$
 (40)

where P(n) is given in units of $[10^{34} \text{ N/m}^2]$ for n in the density range of 0.1 fm⁻³ < n < 3.6 fm⁻³.

For our non-relativistic equation of state (BEHOØ-nr) we find that the following equations of state are the best to cover the whole range of densities in a neutron star, and we use:

HZD in the density range of

$$n < 0.000256$$
,

BBP-1 in the density range of

$$0.000256 \le n < 0.003892$$

BBP-2 in the density range of

$$0.003892 \le n < 0.08$$
,

BEHOØ-nr in the density range of

$$0.08 \le n < 0.8$$
,

 $A\emptyset$ -5 in the density range of

$$0.8 \le n < 3.46$$
,

and PS in the density range of

$$n \ge 3.46$$
,

where n is given in units of [fm⁻³].

For our relativistic equation of state (BEHOØ-r), we have coupled the following equations of state:

HZD in the density range of

$$n < 0.000256$$
,

BBP-1 in the density range of

$$0.000256 \le n < 0.003892$$

BBP-2 in the density range of

$$0.003892 \le n < 0.115$$
,

BEHOØ-gr in the density range of

$$0.115 \le n < 0.7$$

and PS in the density range of

where n is given in units of $[fm^{-3}]$. These equations are chosen among 12 published equations of state, and they seem to be the best ones coupled together in the total density range. Total masses, radii, moments of inertia and surface gravitational redshifts are then calculated, and parameterized as functions of the central density n_c . Table 1 gives results related to our non-relativistic equation of state and table 2 gives results for the relativistic case. In both tables column 1 refers to the central density of the neutron star, column 2 to the total mass, column 3 to the radius, column 4 to the moment of inertia, and column 5 refers to the gravitational redshift. Fig. 2 shows the total mass and fig. 3 the radius versus the central density. Fig. 4 shows the mass versus the radius. Fig. 5 shows the moment of inertia and fig. 6 the gravitational redshift versus the total mass of the star.

4 Discussions and conclusions

From table 1, table 2, and figs. 2–4 we find a maximum mass of

$$M_{\rm max} \approx 1.46 M_{\odot}$$

at a central density of $n_c \approx 2.15 \text{ fm}^{-3}$ with a radius $R \approx 7.45 \text{ km}$ for our non-relativistic equation of state. The maximum mass for our relativistic equation of state is

$$M_{\rm max} \approx 2.37 M_{\odot}$$

at a central density of $n_c \approx 0.8 \text{ fm}^{-3}$ with a radius $R \approx 12.12 \text{ km}$. These results agree very well with "experimental results" from observations of binary pulsars, which give neutron star masses of [30,32]

$$1.0M_{\odot} < M_{\rm max} < 2.2M_{\odot}$$

or possibly [16,33,34]

$$1.4M_{\odot} < M_{\text{max}} < 1.85M_{\odot},$$

Table 1 Neutron star observables as functions of the central density n_c obtained with the non-relativistic equation of state (BEHOØ-nr). M is the total mass, R the radius, I the moment of inertia and Z_s the gravitational redshift.

$n_c [\mathrm{fm}^{-3}]$	$M[M_{\odot}]$	$R[\mathrm{km}]$	$I[10^{38}\mathrm{kg~m^2}]$	Z_s
0.500	0.580	10.18	0.311	0.011
0.650	0.789	9.877	0.453	0.144
0.800	0.957	9.641	0.567	0.189
0.950	1.113	9.332	0.663	0.243
1.100	1.230	9.057	0.730	0.292
1.250	1.312	8.807	0.769	0.336
1.400	1.369	8.570	0.787	0.376
1.550	1.408	8.339	0.790	0.412
1.700	1.434	8.111	0.781	0.447
1.850	1.449	7.887	0.763	0.479
2.000	1.457	7.665	0.739	0.510
2.150	1.458	7.450	0.711	0.539
2.300	1.453	7.241	0.681	0.567
2.450	1.444	7.041	0.649	0.592
2.600	1.431	6.885	0.617	0.615
2.750	1.416	6.681	0.586	0.635
2.900	1.399	6.521	0.556	0.652
3.050	1.381	6.377	0.528	0.666
3.200	1.363	6.247	0.502	0.677
3.350	1.344	6.132	0.477	0.684
3.425	1.335	6.077	0.466	0.687

Table 2 Neutron star observables as functions of the central density n_c obtained with the relativistic equation of state (BEHOØ-r). M is the total mass, R the radius, I the moment of inertia and Z_s the gravitational redshift.

	$n_c [\mathrm{fm}^{-3}]$	$M[M_{\odot}]$	R [km]	$I[10^{38}\mathrm{kg~m^2}]$	Z_s
-					
	0.500	2.227	13.41	3.431	0.401
	0.650	2.356	12.74	3.412	0.485
	0.800	2.370	12.14	3.169	0.538
	0.950	2.337	11.60	2.880	0.572
	1.100	2.286	11.16	2.607	0.591
	1.175	2.258	10.97	2.482	0.598
	1.250	2.229	10.79	2.367	0.602
	1.400	2.173	10.49	2.161	0.606
	1.550	2.120	10.23	1.986	0.605
	1.700	2.070	10.01	1.838	0.603
	1.850	2.025	9.833	1.713	0.596
	2.000	1.983	9.679	1.606	0.591
	2.150	1.946	9.551	1.515	0.584
	2.300	1.912	9.442	1.437	0.577
	2.450	1.881	9.351	1.370	0.570
	2.600	1.853	9.272	1.312	0.562
	2.750	1.827	9.208	1.261	0.555
	2.900	1.805	9.155	1.218	0.547
	3.050	1.784	9.111	1.180	0.540
	3.200	1.766	9.076	1.147	0.533
	3.350	1.749	9.045	1.118	0.527
	3.425	1.741	9.033	1.105	0.524



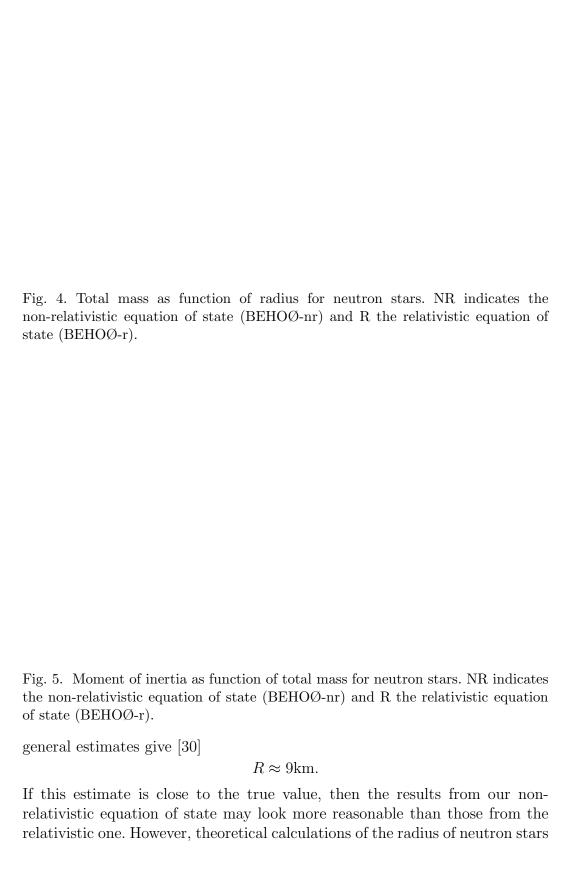


Fig. 6. Surface gravitational redshift as function of total mass for neutron stars. NR indicates the non-relativistic equation of state (BEHOØ-nr) and R the relativistic equation of state (BEHOØ-r).

can not be confirmed very well by observational data, and are more dependent than the total mass on the low-density equation of state.

From table 1, table 2, and fig. 5 we see that our models give a value of

$$I(M_{\text{max}}) = 0.71 \times 10^{38} \text{kgm}^2$$

for the moment of inertia of a neutron star of maximum mass and for the non-relativistic equation of state, and

$$I(M_{\text{max}}) = 3.17 \times 10^{38} \text{kgm}^2,$$

for the relativistic equation of state, while

$$I_{\text{max}} = 0.80 \times 10^{38} \text{kgm}^2,$$

and

$$I_{\text{max}} = 3.47 \times 10^{38} \text{kgm}^2,$$

for our non-relativistic and relativistic equations of state, respectively. These values are not contradictory to observations, and are consistent with the expansion of the Crab nebula and the luminosity and the loss of rotational energy from the Crab pulsar [35].

From fig. 6 we see that the gravitational surface redshift is not strongly affected by the different equations of state. This is because the density profiles of the stars are such that their surface gravities are almost the same. A measurement of the redshift can therefore not be used to distinguish between different types

of stars or equations of state. It is, however, possible that the slowing down of pulsars and the corresponding glitches can give some information about the internal structure.

For some other compact astrophysical objects like, for example, white dwarfs or supermassive black holes in galactic nuclei, theoretical calculations of mass, radius, etc. can provide constraints on physical models. Theoretical calculations for neutron stars, however, can not really give such information due to uncertainties of their internal structure. Instead, we may obtain some information about the nuclear physics of the interior of the star.

Data on the nuclear equation of state can, in principle, be obtained from several different sources such as the monopole resonance in nuclei, high energy nuclear collisions, supernovae, and neutron stars. Until recently it has, for instance, been assumed that the compression modulus was reasonably well known from the analysis of the giant monopole resonance in nuclei [36–38]. Later, however, these results were questioned by the authors of ref. [16,39].

Supernova simulations seem to require an equation of state which is too soft to support some observed masses of neutron stars, if sufficient energy shall be released to make the ejection mechanism work [40–42]. Supernova explosions can then probably not give a reliable constraint on the nuclear equation of state. Some analyses of high energy nuclear collisions, however, have indicated a moderately stiff or very stiff equation of state [43–45], although ambiguities have been observed [46,47]. Various nuclear data and neutron star masses then seem to favour a rather high compression modulus of $K \sim 300~{\rm MeV}$ [16,48,49]. No definite statements can be made, however, about the equation of state at high densities, except that the neutron star equation of state should probably be moderately stiff to support neutron star masses up to approximately 1.85 M_{\odot} [34].

With the above observations, one may be tempted to state that our relativistic EOS is too stiff, since the predicted mass $M_{max} \approx 2.37 M_{\odot}$ and radius are larger than the estimated values. However, there are several mechanisms which serve to soften a given EOS. Amongst these, pions may be likely to condense in neutron star matter, favoured by charge neutrality because neutrons at the top of the Fermi sea could decay to protons plus electrons. Condensation then could possibly occur if the pion energy becomes degenerate with the normal state, but the real situation is still not clear [51]. Also, kaon condensation through the s-wave interaction of kaons with nucleons may be energetically favourable in the interior of neutron stars [52,53]. Kaon condensation would, like pion condensation, increase the proton abundance of matter [51], and could cause a rapid cooling of neutron stars via the direct URCA process. Kaon condensed neutron star cores may also undergo a phase transition to strange quark matter, and neutrino trapping in newly formed neutron star matter could shift

both the kaon condensation and the quark matter transition to higher densities. The equation of state for neutron stars would be softened considerably due to pion or kaon condensation because of the lower symmetry energy of nuclear matter, and maximum masses are then reduced correspondingly from the cases with no condensates. This should have important implications for the formation of black holes in stellar collapse, and the number of black holes in the Galaxy should then be substantially higher than estimated earlier.

Further processes which can soften the equation of state are also conversion of nucleons to hyperons or a phase transition to quark matter at high densities, which would both lower the energy by an increase in the number of degrees of freedom. However, for a neutron star to resist the centrifugal forces from very fast rotation, the equation of state should be soft at low and intermediate densities and stiff at high densities, which would not fit very well with the concept of quark matter in hybrid stars [17].

In summary, in this work we have calculated the EOS for neutron matter using the recent meson-exchange potential models of the Bonn group. Both a non-relativistic and a relativistic Brueckner-Hartree-Fock procedure were employed in order to derive the equation of state, which is the basic input quantity in neutron star calculations since it connects the nuclear physics and the astrophysics. Of importance here is the fact that a relativistic nuclear matter calculation with the Bonn A potential [13] meets the empirical nuclear matter data, a feature not accounted for by non-relativistic calculations. The relativistic effects become important at densities around and higher than the saturation density for nuclear matter, and their main effect is to stiffen the EOS at these densities. This mechanism is due to the fact that the relativistic effective mass of the nucleon becomes smaller compared to the free mass, an effect which in turn enhances the repulsive spin-orbit term.

Albeit the description of the matter inside the star is a complicated many-body problem, we have in this work used equations of state for neutron matter only, in order to assess the importance of relativistic effects in neutron star calculatons. Our conclusions are that the relativistic EOS yields too stiff an EOS, however, many-body effects not included here, may soften the EOS and bring the relativistic results close to the empirical values for mass and radius. The other observables like moment of inertia and gravitational redshifts are in good agreement with the accepted values.

Many discussions with Ruprecht Machleidt on the Dirac-Brueckner approach are greatly acknowledged.

References

- [1] C.J. Pethick and D.G. Ravenhall, Phil. Trans. Roy. Soc. Lond. A341 (1992) 17
- [2] F. Weber and N.K. Glendenning, *Hadronic matter and rotating relativistic neutron stars*, (World Scientific, Singapore, in press)
- [3] C.J. Pethick, Rev. Mod. Phys. **64** (1992)1133
- [4] R. Machleidt, Adv. Nucl. Phys. **19** (1989) 189
- [5] R. Machleidt and G.Q. Li, to appear in Physics Reports
- [6] S.D. Serot and J.D. Walecka, Adv. Nucl. Phys. **16** (1986) 1
- [7] R.B. Wiringa, V. Fiks and A. Fabrocini, Phys. Rev. C38 (1988) 1010
- [8] W.H. Dickhoff and H. Müther, Rep. Prog. Phys. **55** (1992) 1947
- [9] T.T.S. Kuo and Z.Y. Ma, Phys. Lett. B127 (1983) 123; T.T.S. Kuo and Z.Y. Ma, in Nucleon-Nucleon Interaction and Nuclear Many-body Problems (edited by S.S. Wu and T.T.S. Kuo) (World Scientific: Singapore) p. 178; T.T.S. Kuo, Z.Y. Ma and R. Vinh Mau, Phys. Rev. C33 (1986) 717
- [10] L. Ray, G.W. Hoffman and W.R. Cooker, Phys. Rep. **212** (1991) 223
- [11] T. Nikolaus, T. Hoch and D.G. Madland, Phys. Rev. C46 (1992) 1757
- [12] R. Brockmann, Phys. Rev. C18 (1978) 1510
- [13] R. Brockmann and R. Machleidt, Phys. Rev. C42 (1990) 1965
- [14] H. Müther, R. Machleidt and R. Brockmann, Phys. Rev. C42 (1990) 1981
- [15] G.Q. Li, R. Machleidt and R. Brockmann, Phys. Rev. C46 (1992) 2782
- [16] N.K. Glendenning, Phys. Rev. C37 (1988) 2733
- [17] F. Weber, N.K. Glendenning and M.K. Weigel, Astrophys. Journ. 373 (1991) 579
- [18] C. Mahaux and R. Sartor, Phys. Rev. C 40 (1989) 1833; C. Mahaux, P.E. Bortignon, R.A. Broglia and C.H. Dasso, Phys. Rep. 120 (1985) 1
- [19] H.Q. Song, S.D. Yang and T.T.S. Kuo, Nucl. Phys. **A462** (1987) 491
- [20] M.F. Jiang, R. Machleidt and T.T.S. Kuo, Phys. Rev. C41 (1989) 2346; M.F. Jiang, T.T.S. Kuo and H. Müther, Phys. Rev. C40 (1989) 1836
- [21] L.S. Celenza and C.M. Shakin, *Relativistic Nuclear Physics: Theories of Structure and Scattering*, Vol. 2 of Lecture Notes in Physics, (World Scientific, Singapore, 1986)
- [22] B. ter Haar and R. Malfliet, Phys. Rep. **149** (1987) 207

- [23] C.J. Horowitz and B.D. Serot, Nucl. Phys. **A464** (1987) 613
- [24] B.D. Serot, Rep. Prog. Phys. **55** (1992) 1855
- [25] R.H. Thompson, Phys. Rev. **D1** (1970) 110
- [26] C. Itzykson and J.-B. Zuber, *Quantum Field theory*, (McGraw-Hill, New York, 1980)
- [27] L. Engvik, M. Hjorth-Jensen, T.T.S. Kuo and E. Osnes, to be published
- [28] P. Haensel, J.L. Zdunik and J. Dobaczewski, Astron. Astrophys. 222 (1989) 353
- [29] G. Baym, H.A. Bethe and C.J. Pethick, Nucl. Phys. A175 (1971) 225
- [30] T. Øvergård and E. Østgaard, Can. Journ. Phys. **69** (1991) 8
- [31] V.R. Pandharipande and R.A. Smith, Nucl. Phys. **A237** (1975) 507
- [32] M. Prakash, T.L. Ainsworth and J.M. Lattimer, Phys. Rev. Lett. 61 (1988) 2518
- [33] J.H. Taylor and J.M. Weisberg, Astrophys. Journ. 345 (1989) 434
- [34] P.C. Joss and S.A. Rappaport, Ann. Rev. Astron. Astrophys. 22 (1984) 537
- [35] T. Mølnvik and E. Østgaard, Nucl. Phys. A437 (1985) 239
- [36] J.P. Blaizot, D. Gogny and B. Grammiticos, Nucl. Phys. **A265** (1976) 315
- [37] J.P. Blaizot, Phys. Rep. **64** (1980)171
- [38] J. Treiner, H. Krevine, O. Bohigas and J. Martorell, Nucl. Phys. A317 (1981) 253
- [39] G.E. Brown and E. Osnes, Phys. Lett. **B159** (1985) 223
- [40] E. Baron, J. Cooperstein and S. Kahana, Phys. Rev. Lett. **55** (1985) 126
- [41] S.E. Woosley and T.A. Weaver, Ann. Rev. Astron. Astropys. 24 (1986) 205
- [42] E. Baron, H.A. Bethe, G.E. Brown, J. Cooperstein and S. Kahana, Phys. Rev. Lett. 59 (1987) 736
- [43] M. Sano, M. Gyulassy, M. Wakai and Y. Kitazoe, Phys. Lett. **B156** (1985) 27
- [44] H. Stocker and W. Greiner, Phys. Rep. **137** (1986) 277
- [45] J.J. Molitoris, D. Hahn and H. Stocker, Nucl. Phys. A447 (1985) 13c
- [46] C. Gale, G. Bertsch and S. Das Gupta, Phys. Rev. C35 (1987) 415
- [47] J. Aichelin, A. Rosenhauer, G. Peilert, H. Stocker and W. Greiner, Phys. Rev. Lett. 58 (1987) 1926

- [48] M.M. Sharma, W.T.A. Borghols, S. Brandenburg, S. Crona, A. van der Woude and M.N. Harakeh, Phys. Rev. C38 (1988) 2562
- [49] M.M. Sharma, W. Stocker, P. Gleissl and M. Brack, Nucl. Phys. A504 (1989) 337
- [50] F. Weber and N.K. Glendenning, Astrophys. Journ. 390 (1992) 541
- [51] R. Mittet and E. Østgaard, Phys. Rev. C37 (1988) 1711
- [52] V. Thorsson, M. Prakash and J. Lattimer, NORDITA preprint, no. 29 (1993)
- [53] G.E. Brown, C.-H. Lee, M. Rho and V. Thorsson, NORDITA preprint, no. **30** (1993)